Vol 14 No 3, March 2005
1009-1963/2005/14(03)/556-04
Chinese Physics
© 2005 Chin. Phys. Soc.
and IOP Publishing Ltd

Effect of void formation during MEVVA tungsten ion implantation on the microstructure and surface properties of H13 die steel*

Yang Jian-Hua(杨建华)[a)b)c)†] and Zhang Tong-He(张通和)[c)]

[a)] *Department of Physics, Nantong University, Jiangsu* 226007, *China*
[b)] *Key Lab of ASIC Design, Nantong University, Jiangsu* 226007, *China*
[c)] *Radiation Beam and Materials Engineering Lab, Beijing Normal University, Beijing* 100875, *China*

(Received 15 July 2004; revised manuscript received 6 September 2004)

H13 die steel was implanted with tungsten using a metal vapour vacuum arc (MEVVA) ion source. When the pulsed beam current density of tungsten ions increased to 6mA·cm^{-2}, some voids appeared in the high voltage electron microscope (HVEM) micrograph, which would disappear at an annealing temperature of 600°C. HVEM and x-ray diffraction were used for observing the phase structure of the annealed and un-annealed H13 steel after the steel was implanted. Results of wear and hardness tests indicated that whether the voids appear significantly influences the hardness and wear of H13 steel. Reasons for the formation of voids and the relation between the surface mechanical property and voids are discussed in terms of collision theory.

Keywords: ion implantation, annealing, void, wear, MEVVA
PACC: 5250D, 6170Q, 6170W, 6220, 8140P

1. Introduction

Ion implantation is a method for modifying the surface composition and microstructure of materials so as to improve the wear and corrosion resistance.[1−4] Since the development of high current metal ion sources such as metal vapour vacuum arc (MEVVA), the metallurgical ion implantation of metal species has been emerging as a potentially affordable technique for civil application.[5−7] One of the key issues for successful accomplishment of industrial applications should be the selection of ion species and the optimization of their implantation parameter.[8−13] The higher the ion current density is, the shorter the implantation time for reaching certain implantation dose. However, it is not too clear how a high ion current density influences implantation effect. In this paper, we study the tribological change of W-implanted H13 steel depending on variation in W ion current density. We found that voids induced by tungsten ion implantation at high ion current density could increase the hardness and wear of H13 steel. The voids were found to disappear at an annealing temperature of 600°C, which improves the wear resistance of the implanted H13 steel. In addition, the relationship between surface mechanical properties and microstructure is discussed.

2. Experimental methods

The samples were made from hot extruded die steel H13 (0.36wt%C, 5.7wt%Cr, 1.6wt%Mo, 1.1wt%V, 0.8wt%Si, 0.2wt%Mn) in the form of square discs of 12mm×12mm ×1.5 mm (thick samples for tribology testing) and 12mm×12mm ×0.1 mm (thin samples for high voltage electron microscope (HVEM) experiments). All of the samples were polished to a metallographic finish and quenched at 1050°C for an hour and then annealed at 500°C for an hour before ion implantation. A MEVVA source can produce multicharge state ions. The percentages of the tungsten ions with 1 to 5 elementary charges measured by a time of flight were 6%, 40%, 36%, 13% and 5%, respectively. The tungsten ions were implanted into H13 steel at an acceleration voltage of 30kV, corresponding to an average ion energy of about 81keV since the average charge state of tungsten ions mea-

*Project supported by the National Natural Science Foundation of China (Grant No 59671051) and Nantong University.
†E-mail: yang.yangyangj@163.com

sured was about 2.7. The pulsed beam flux of W ion was between 0.3 and 6mA·cm^{-2}. The dose of tungsten ions was 1×10^{17}cm^{-2}. During the implantation, the samples were fixed on a water-jacketed iron plate in a vacuum chamber to keep their temperature below 200°C. The hardness was measured by a Vickers hardness sclerometer with a load of 2.5g. A pin-on-disc apparatus with a pin was used for wear testing at a velocity of 16mm·s^{-1}. The applied normal load of wear testing was 20g. The wear tests were continued to 800 circles. The average maximal depth (D), the average width (W) and $S(= D \times W/2)$ of wear tracks were measured by an optical interference microscope. Since all the experiment conditions were the same for the unimplanted steel and implanted steel, the S of wear tracks are directly proportional to the wear rate. The surface compositions of implanted layers were measured by Rutherford backscattering spectrum (RBS). For the RBS measurement, 2.0MeV alpha particles were normally incident onto the samples, with the backscattering ions being detected at an angle of 165°. X ray diffraction (XRD) and HVEM were used for observing the phase structure of the annealed and un-annealed samples after ion implantation. XRD measurements were carried out on a Rigaku D/max-RB diffractometer, with the grazing incidence geometry, using Cu Kα radiation. The incident x-ray beam is 5° with respect to the sample surface. Specimens for HVEM at 1MV were prepared by ion milling from the unimplanted side. First the samples were observed in HVEM at room temperature (RT). Then the specimen with voids was heated up to 600°C step by step in HVEM. During the heating process we looked at the screen to observe the change of morphology in the same area of the thin film and took a bright field image and its diffraction pattern. To avoid the effect of electron irradiation the area chosen to take a bright field image and its diffraction pattern was moved out of the observation screen during the heating process.

3. Experimental results and discussions

3.1. HVEM results

The microstructure of the unimplanted sample as shown by HVEM has a martensite structure, and the electron diffraction pattern was made up of α-Fe diffraction spots due to big crystal grains of H13 steel (Fig.1(a)). A highly dense uniform damage layer appeared in the HVEM micrograph instead of the martensite structure after implantation at a pulsed ion beam flux of 0.3A·cm^{-2}. The electron diffraction pattern showed widened diffraction rings corresponding to α-Fe (Fig.1(b)). In addition, there were some dotted weak rings corresponding to tungsten carbide (WC) in the electron diffraction pattern, in accord with the corresponding XRD results. When the pulsed ion beam current density increased to 6mA·cm^{-2}, some voids with a diameter of about 30nm appeared on the HVEM micrograph and the electron diffraction pattern showed diffuse diffraction halo-rings corresponding to α-Fe, which implied that an amorphous zone had formed (Fig.1(c)). Meanwhile, the dotted rings corresponding to WC hardly appeared in this case. The diameters of the voids were not changed at annealing temperature lower than 200°C. However, the voids disappeared when the annealing temperature rose to 600 °C and held for 20 minutes. (Fig.1(d))

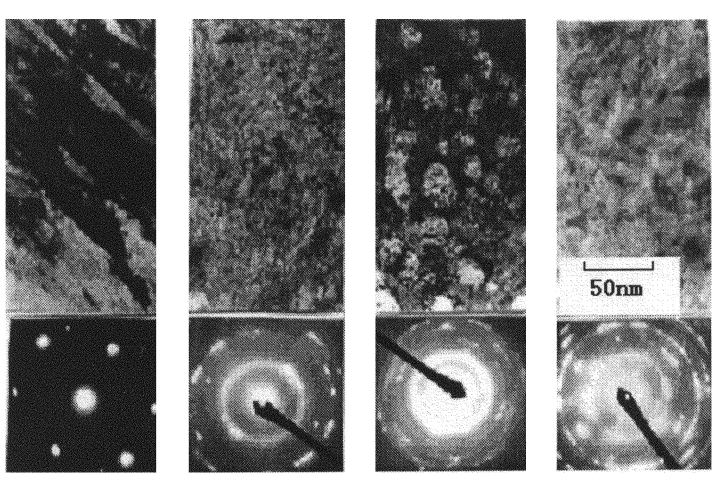


Fig.1. HVEM images and diffraction patterns of the implanted and unimplanted steel. (a)-unimplanted (RT), (b)-0.3 mA·cm^{-2}(RT), (c)-6mA·cm^{-2}(RT), (d)-6mA·cm^{-2}(600°C annealing).

3.2. XRD analysis

The XRD spectrum from the unimplanted H13 steel sample is given in Fig.2(a). There were two peaks in the XRD spectrum. The spectrum was the same as that of the pure Fe in spite of Cr concentration of 5.7 wt% in H13 steel according to PDF card. The XRD spectrum of the sample tungsten implanted at 0.3mA·cm^{-2} is shown in Fig.2(b). It can be seen from Fig.2(b) that the diffraction peaks of WC could be detected, though the intensity of the diffraction peaks was much lower than that of the Fe (110) peak. The XRD spectrum from H13 steel implanted at 6mA·cm^{-2} was quite similar to that of the unimplanted one, while annealing made the peaks belonging to WC to appear again (Fig.2(c)). The Miller indices of the peaks from the unimplanted and implanted steel are marked in Fig.2.

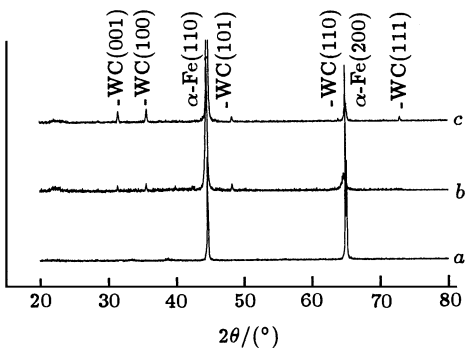


Fig.2. The XRD of implanted and unimplanted steel *a*-unimplanted (RT), *b*-0.3 mA·cm^{-2} (RT), *c*-6mA·cm^{-2} (600°C annealing).

3.3. Wear resistance measurement

For wear testing, interferograms of wear tracks of implanted and unimplanted H13 steel were obtained with an optical interference microscope. The hardness was measured by a Vickers hardness sclerometer. Table 1 shows these measured results.

Table 1. The values S and hardness of implanted and unimplanted H13 steel.

sample	ion current density /(mA·cm^{-2})	Hardness /(kg·mm^{-2})	S /(10^{-4}mm^2)	Target temperature/°C	Annealing temperature/°C
a	(unimplanted)	550	3.8		RT
b	0.3	750	1.6	150	RT
c	6	1150	4.1	180	RT
d	6	850	2.6	180	600

This indicated that tungsten ion implantation could obviously improve the wear resistance of the implanted samples when the ion current density of W ion implantation was 0.3 mA·cm^{-2}, while the wear would increase when the ion current density rose to 6mA·cm^{-2}. In addition, annealing could improve the wear resistance of the sample implanted at the ion current density of 6mA·cm^{-2}. Besides the value of S, ion implantation dramatically altered the texture of wear tracks in dry sliding. Some debris-like plates could be observed in the unimplanted track. The track of implanted sample showed very little damage when ion current density was 0.3 mA·cm^{-2}. From these results, it could be considered that the wear mode of the tungsten-implanted sample was in a plough mode in 800 circles because the track was only made up of shallow and narrow grooves. The unimplanted sample has already been in a shearing mode when wear tests were continued to 800 circles because some debris-like "plates" have appeared in the unimplanted track. Obviously tungsten ion implantation could make the shearing wear of the steel to be delayed when the ion current density of implantation was 0.3 mA·cm^{-2}. Bigger debris than that on the unimplanted track appeared on the corresponding track when the pulsed ion beam current density increased to 6mA·cm^{-2}.

3.4. RBS analysis

The concentration depth profiles of tungsten atoms in H13 steel were obtained from RBS (Fig.3). They were different from the distribution of monoenergetic incident ion in steel at a low dose, probably owing much to diffusion and the higher percentage of ions with 2 and 5 elementary charges. It could be shown that the maximum percentage concentration of tungsten atoms was about 10% for the tungsten ion implantation. Because of sputtering, the position of tungsten maximal concentration was near the surface of the implanted samples. The retained dose was much bigger than what is calculated by normal collision theory[14] due to beam heating, high beam flux and radiation enhanced diffusion. The thickness of the implanted layer for the implantation, in which relative atomic concentration was greater than 4%, was twice

that calculated by normal collision theory.[14] The thickness of the modification layer was about 1 μm because the thickness of the modification layer is usually 10 times greater than that of the implanted one.[15] The W concentration depth distributions in the unannealed H13 steel ,which had been implanted at the ion current density of 6mA·cm^{-2}, was not shown because there would be great error in the concentration depth profiles from RBS due to the existence of the voids.

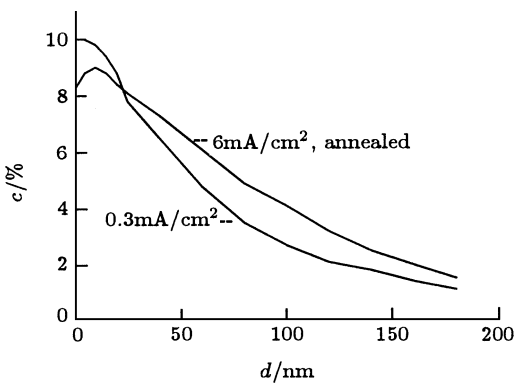


Fig.3. *W* concentration depth profile in H13 steel.

3.5. Discussion

Although further quantitative analysis is needed, a qualitative understanding of the contribution of ion implantation to hardening can be provided by the HVEM, XRD, RBS and collision theory. A W ion is much heavier than a Fe atom. When a W ion with an energy lower than 100keV strikes the atoms of H13 steel, a nonlinear cascade collision will result and may produce a corresponding melting zone in the steel which is usually referred to as a "spike".[1,16] The melting zone was then considered to cool via thermal conduction to the surroundings and crystallization was considered feasible. The melting zone may become amorphous due to fast cooling velocity. The H13 steel with amorphous surface may reduce the shearing wear and improve the wear resistance of the implanted steel.[17] Further, the melting zone may even be boiled away because a new particle (ion or recoiled atom) may pass through it at a higher ion current density during re-crystallization. Therefore, a void may form as the relic of the spike quenching. Once a void has formed, a W ion implanted subsequently can implant deeper while the surface concentration of implanted ions would decrease. Although the void formed may increase the strain of the implanted layer and hardness, it can become the source of some crackle, make wear debris form and deteriorate the wear resistance of the implanted steel. The annealing at 600°C can make the voids disappear and decrease sources of crackle, which will improve the wear resistance of the H13 steel. Many studies did not discover the void forming due to using lower ion current density usually.

4. Conclusions

Tungsten ion implantation at 30kV, corresponding to the average ion energy of about 81keV, can improve the wear resistance of H13 steel significantly when the ion current density of W ion implantation was 0.3mA·cm^{-2}.

Voids induced by ion implantation can increase hardness and wear of H13 steel at a high ion current density at 6mA·cm^{-2}. The annealing at 600°C can make the voids disappear and improve its wear resistance after H13 steel was implanted.

Acknowledgements

The authors wish to thank Zhang Huixing for the ion implantation (Beijing Normal University) and Wang Xuemei for the RBS (Beijing University).

References

[1] Cheng Y 1990 *Mater. Sci. Rep.* **5** 45
[2] Wang J, Zhang G, Liu Y, Wang Y, Liu C and Yang S 2004 *Chin. Phys.* **13** 65
[3] Xu F, Chen G, Yang Q, Ye M and Li Y 2001 *Chin. Phys.* **10** 1049
[4] Wolf G 1996 *Surf. Coat. Tech.* **83** 1
[5] Treglio J *et al* 1989 *Nucl. Instrum. Methods* **B40/41** 567
[6] Brown I G *et al* 1988 *J. Appl. Phys.* **63** 4899
[7] Yang J and Zhang T 2004 *Acta Phys. Sin.* **53** 3823 (in Chinese)
[8] Sharkeev Y P, Gritsenko B P, Fortuna S V A and Perry J 1999 *Vacuum* **52** 247
[9] Manory R R, Mollica S and Ward L 2002 *Surf. Coat. Tech.* **115** 136
[10] Wang X, Chen M, Dong Y, Chen J, Wang X and Liu X 2002 *Surf. Coat. Tech.* **158–159** 180
[11] San J, Liu J, Zhu B, Mo Z, Zhang Q and Dong C 2002 *Surf. Coat. Tech.* **161** 1
[12] Han B, Zhang H, Zhao W, Yan S, Le X, Xiang W, Wang T and Remnev G 2002 *Surf. Coat. Tech.* **158–159** 482
[13] Cheng X, Tang X and Liu B 2004 *J. Alloys Compounds* **365** 240
[14] Schulz F 1976 *Rad. Eff.* **29** 31
[15] Singer I L and Jeffries R A 1984 *Mater. Res. Soc. Symp. Proc.* **27** 667
[16] Bibic N, Dhar S, Milosavljevic M *et al* 2000 *Nucl. Instrum. Methods* B **161–163** 1011
[17] Zhang T 2002 *Chin. Phys.* **11** 272